JOURNAL OF THE ROYAL SOCIETY Interface

The enzyme aromatic amine dehydrogenase induces a substrate conformation crucial for promoting vibration that significantly reduces the effective potential energy barrier to proton transfer

Linus O Johannissen, Nigel S Scrutton and Michael J Sutcliffe

J. R. Soc. Interface 2008 **5**, 225-232
doi: 10.1098/rsif.2008.0068.focus

Interface focus

J. R. Soc. Interface (2008) **5**, S225–S232
doi:10.1098/rsif.2008.0068.focus
Published online 21 May 2008

The enzyme aromatic amine dehydrogenase induces a substrate conformation crucial for promoting vibration that significantly reduces the effective potential energy barrier to proton transfer

Linus O. Johannissen[1], Nigel S. Scrutton[2] and Michael J. Sutcliffe[1,*]

[1]*School of Chemical Engineering and Analytical Science, and* [2]*Faculty of Life Sciences, and Manchester Interdisciplinary Biocentre, University of Manchester, 131 Princess Street, Manchester M1 7DN, UK*

The role of promoting vibrations in enzymic reactions involving hydrogen tunnelling is contentious. While models incorporating such promoting vibrations have successfully reproduced and explained experimental observations, it has also been argued that such vibrations are not part of the catalytic effect. In this study, we have employed combined quantum mechanical/molecular mechanical methods with molecular dynamics and potential energy surface calculations to investigate how enzyme and substrate motion affects the energy barrier to proton transfer for the rate-limiting H-transfer step in aromatic amine dehydrogenase (AADH) with tryptamine as substrate. In particular, the conformation of the iminoquinone adduct induced by AADH was found to be essential for a promoting vibration identified previously—this lowers significantly the 'effective' potential energy barrier, that is the barrier which remains to be surmounted following collective, thermally equilibrated motion attaining a quantum degenerate state of reactants and products. When the substrate adopts a conformation similar to that in the free iminoquinone, this barrier was found to increase markedly. This is consistent with AADH facilitating the H-transfer event by holding the substrate in a conformation that induces a promoting vibration.

Keywords: hydrogen tunnelling; kinetic isotope effect; molecular dynamics; promoting vibrations

1. INTRODUCTION

1.1. Role of dynamics in catalysis

Enzyme catalysis is inherently a dynamic process with the catalytic step involving atomic fluctuations along the reaction coordinate, which lead to bonds being broken and new ones formed. Proteins undergo a wide range of motions in terms of time (10^{-15} to more than 1 s) and distance (10^{-2} to greater than 10 Å) scales: sub-picosecond atomic vibrations, pico- to nanosecond backbone and side chain motions, millisecond conformational rearrangements and slow 'breathing modes' of the order of seconds (Yon *et al.* 1998; Henzler-Wildman & Kern 2007). Any of these motions may be functionally significant and directly related to catalysis. Although we understand that enzymes (and more generally proteins) are dynamic molecules, the overriding picture that emerges from structural biology is a static one. Protein structures determined from X-ray crystallography and NMR spectroscopy have provided important insight into the form and function of enzymes, yet they give only brief snapshots into the life of a protein—very little is known about dynamic processes that trigger catalysis. Static protein structures show only the lowest energy or 'groundstate' conformation and the time averaged conformational ensemble, yet multiple protein conformations may exist in thermal equilibrium and function may depend on excursions to sparsely populated higher energy conformations of the enzyme and its substrates. Moreover, there is increasing recognition of the importance of non-equilibrated fast (sub-picosecond) dynamics in modifying the free energy barrier for a reaction (Caratzoulas *et al.* 2002; Knapp *et al.* 2002; Garcia-Viloca *et al.* 2003; Masgrau *et al.* 2006; Dybala-Defratyka *et al.* 2007; Hay *et al.* 2007; Johannissen *et al.* 2007), which by definition influence the rate of an enzyme-catalysed reaction. There is poor

*Author for correspondence (mike.sutcliffe@manchester.ac.uk).

Electronic supplementary material is available at http://dx.doi.org/10.1098/rsif.2008.0068.focus or via http://journals.royalsociety.org.

One contribution of 9 to a Theme Supplement 'Biomolecular simulation'.

Received 12 February 2008
Accepted 23 April 2008

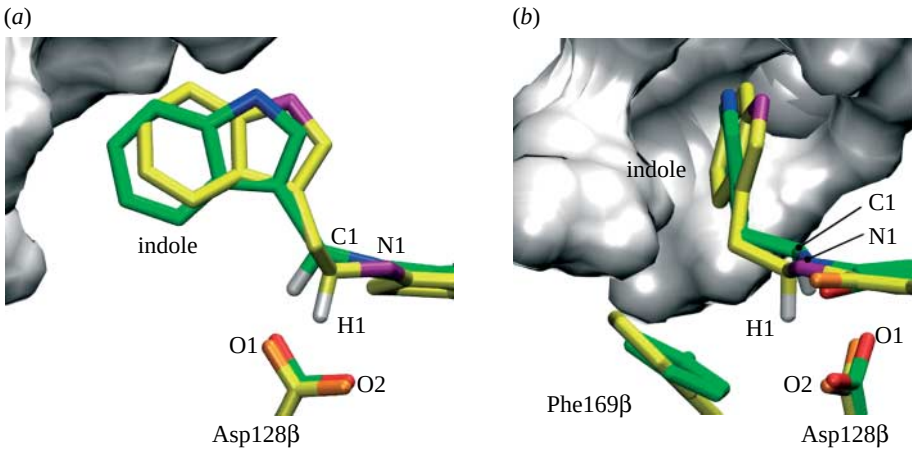

Figure 1. Active site of QM/MM minimized AADH with bound iminoquinone from (*a*) the $\alpha_2\beta_2$-heterotetramer (green carbon atoms) and (*b*) the isolated β-monomer (yellow carbon atoms), overlaid on the quinone plus backbone heavy atoms of the residues shown. The grey surface represents the α-subunit residues from the $\alpha_2\beta_2$-heterotetramer within 5 Å of the iminoquinone.

understanding of structural change associated with this motion owing to the technical limitations of current structural biology methods (Wand 2001).

1.2. Computational studies of H-transfer

Computational studies provide essential atomistic insight into the mechanism of H-transfer (Pu *et al.* 2006). Despite recent advances, such simulations remain challenging owing to the importance of both electronic and nuclear quantum effects as well as the effects of protein motion. The incorporation of electronic quantum effects is required for the description of the breakage and formation of chemical bonds. Nuclear quantum effects, such as zero-point energy and hydrogen tunnelling, are also significant. However, over the past decade, with the enhancements in both computer power and theoretical approaches, computational simulations have become increasingly attractive in the study of hydrogen transfer reactions in enzymes. Agreement between experiment, computation and theory provides powerful evidence in support of environmentally coupled H-tunnelling (Hammes-Schiffer 2006; Kohen 2006; Sutcliffe & Scrutton 2006). Computational simulations have indicated that in a number of enzyme systems H-transfer can occur by a mixture of 'over the barrier' and 'through the barrier' events (Alhambra *et al.* 2001; Billeter *et al.* 2001; Cui & Karplus 2002; Hammes-Schiffer 2006; Pang *et al.* 2006; Pu *et al.* 2006)—in only a few systems is transfer essentially a 'pure' tunnelling process (Masgrau *et al.* 2006; Pu *et al.* 2006; Tejero *et al.* 2006; Pang *et al.* 2008), a so-called deep tunnelling reaction. Simulation has revealed a major role for dynamics in the H-transfer event, in terms of both (i) a collective, thermally equilibrated motion to attain a quantum degenerate state of reactants and products (Benkovic & Hammes-Schiffer 2003), enhancing the probability of tunnelling by increasing the wave function overlap of the reactant and product states and (ii) a fast non-equilibrated 'promoting' motion that modifies the properties of the tunnelling barrier once the degenerate states have been reached (Caratzoulas *et al.* 2002; Masgrau *et al.* 2006) to further enhance the probability of tunnelling (if such an enhancement is required). The existence of 'promoting motions' has been contentious (Ball 2004; Masgrau *et al.* 2006). Indeed, it has been suggested that these vibrational modes may not contribute to the catalytic effect since vibrations that similarly reduce the tunnelling distance are also expected in solution-based reactions, that shortening of the proton–acceptor distance decreases the degree of tunnelling (Olsson *et al.* 2006*a*) and that electrostatic preorganization is the most important factor to enzyme catalysis (Warshel 1998; Olsson *et al.* 2006*b*; Liu & Warshel 2007*a*,*b*). However, combined studies embracing experiment, simulation and numerical analysis have supported the existence of promoting motions in enzyme systems (Hay *et al.* 2007; Johannissen *et al.* 2007).

1.3. Aromatic amine dehydrogenase

The enzyme aromatic amine dehydrogenase (AADH) catalyses the oxidative deamination of primary amines, which involves proton transfer from an iminoquinone intermediate to a catalytic base (Asp128β). We recently published a combined kinetic, crystallographic and computational study of this chemical step in the reaction of tryptamine with AADH. The kinetic data revealed an elevated KIE (approx. 55) with very weak temperature dependence (Johannissen *et al.* 2007), which is strongly indicative of proton transfer by tunnelling. This was further supported by variational transition state theory calculations with multi-dimensional tunnelling corrections (MT-VTST), at least 99% of proton transfers occur by tunnelling through a distance of less than 0.6 Å (Masgrau *et al.* 2006, 2007). These results also showed that, counter-intuitively, the preferred proton acceptor (thermodynamically and kinetically) is the Asp128β carboxyl oxygen, which is located furthest from the donor and transferring proton in the reactant structure. Significant rearrangements in the donor and acceptor atoms are required to achieve a tunnelling-ready configuration, namely a rotation of the donor carbon (C1) such that the transferring proton (H1) moves towards the acceptor (O2), coupled to a repositioning of O2 (see figure 1 for atom labels). The rotation of the donor group causes the secondary hydrogen on C1 to become more in-plane with the iminoquinone and the

C1–H1 bond more perpendicular to it, thus making the sp^3-hybridized donor carbon more sp^2 (product)-like. This partly explains why O2 is the preferred proton acceptor (Johannissen *et al.* 2007).

Molecular dynamics (MD) simulations revealed that the principal motion of the donor methylene group corresponds to this required rotation towards O2, and therefore would facilitate proton transfer (Masgrau *et al.* 2006). Further analysis revealed that this motion is part of an approximately 165 cm^{-1} promoting vibration, in which the motions of C1, H1 and O2 are all coupled to the H-transfer coordinate (Johannissen *et al.* 2007). This promoting vibration is inherent to the iminoquinone intermediate, and not part of a long-range network of coupled vibrations, which suggests that one role the enzyme plays in facilitating this particular tunnelling event is that of a scaffold holding the iminoquinone in position such that the vibration inherent to the donor methylene group aligns with the H-transfer coordinate.

In this study, we have employed combined quantum mechanical/molecular mechanical (QM/MM) calculations to investigate how the dynamics of the enzyme and iminoquinone intermediate affect the reaction profile for the proton transfer from said intermediate to Asp128β in AADH. Important insight was gained from comparisons of the potential energy surfaces (PESs) for the native AADH $\alpha_2\beta_2$-heterotetramer to those for the isolated β-monomer (the tryptophan tryptophylquinone-containing subunit), which has been found to be catalytically active but with a proton transfer rate three orders of magnitude lower than the native $\alpha_2\beta_2$-form (Hothi *et al.* 2008). In particular, the structure of the active site was found to be essential for the promoting vibration, which lowers the effective potential energy barrier of the reaction.

2. METHODS

2.1. Combined QM/MM setup

All calculations reported in this study are combined QM/MM calculations, carried out at the AM1/CHARMM22 level using CHARMM (Brooks *et al.* 1983). The QM region comprises the iminoquinone and Asp128β side chain, linked to the rest of the enzyme by three HQ-type link atoms (Field *et al.* 1990) as described previously (Masgrau *et al.* 2006). For the $\alpha_2\beta_2$-heterotetramer, the starting structure was taken after 2 ns of MM MD simulation (Masgrau *et al.* 2006; Johannissen *et al.* 2007), and that for the isolated β-monomer, for which there is no X-ray crystal or NMR structure available, taken after 5 ns of MM MD simulation of one β-monomer from the energy minimized $\alpha_2\beta_2$-structure. The longer MD simulation for the monomer was required owing to a conformational change (see figure 1 and electronic supplementary material, figure S1), which occurs after approximately 3.5 ns.

2.2. QM/MM MD simulations

Each starting structure taken from the MM MD simulations was first QM/MM energy minimized. Thermalization was then carried out for 12 ps, followed by 220 ps of CPT dynamics, the first 20 ps of which was discarded as equilibration.

2.3. PES calculations

The one-dimensional PESs along the proton-transfer coordinate were calculated on structures sampled during the QM/MM MD simulations (snapshots). The reaction coordinate was defined as

$$z = d(\mathrm{O2-H1}) - d(\mathrm{C1-H1}), \tag{2.1}$$

where H1 is the proton being transferred; C1 is the donor (methylene) carbon; and O2 is the acceptor (carboxyl) oxygen (Masgrau *et al.* 2006). For each snapshot, the QM region was first energy minimized with the value of z restrained and the positions of atoms in the MM region fixed. Energy minimizations were carried out at z intervals of 0.05 Å, using a harmonic restraint of 1000 kcal mol^{-1} $Å^{-2}$ to fix z, for the range $-2\ Å \le z \le 2\ Å$. These calculations also employed a harmonic restraint of 10 kcal mol^{-1} $Å^{-2}$ on the MM region, as previously used in a study of human purine nucleoside phosphorylase (Garcia-Viloca *et al.* 2001), to ensure that structural changes in the protein scaffold that occur during the MD simulation are retained during the PES calculations.

3. RESULTS AND DISCUSSION

3.1. Structural differences between the β-monomer and the $\alpha_2\beta_2$-heterotetramer active sites

Although the isolated β-monomer contains a solvent-exposed active site, the indole ring of the iminoquinone adduct shields the reacting moieties themselves, iminoquinone and Asp128β carboxyl, from solvent exposure (figure 1). Therefore, the most intuitive explanation for the lower proton-transfer rate in the β-monomer would be that H1 and O2 are not held close enough apart for effective proton transfer to take place. However, a 200 ps QM/MM MD simulation of the solvated monomer (initiated after 5 ns of MM MD simulation) suggests that the opposite is in fact true; there is less fluctuation in the C1–H1–O2 distances, and d(O2–H1) lies much more frequently below 2 Å than in the $\alpha_2\beta_2$-heterotetramer (electronic supplementary material, figure S2). This arises because, in the absence of the α-subunit, Phe169β and the indole ring undergo a conformational change (figure 1), with the indole arching over the quinone in a conformation more akin to that in an energy-minimized unrestrained iminoquinone analogue (electronic supplementary material, figure S3*b*). This suggests that the presence of the α-subunit in the native enzyme forces the iminoquinone away from its energetically preferred conformation. This conformational change persists over time (electronic supplementary material, figure S4). The position of the indole in the β-monomer causes the C1–H1 bond to point more towards O2, which would at first glance appear to favour proton transfer. The significance for the transfer of H1 of this new distinct conformation of Phe169β is discussed in §3.4.

3.2. PESs for the $\alpha_2\beta_2$-heterotetramer and β-monomer

PESs were calculated for 200 structures sampled at 1 ps intervals from a 200 ps QM/MM MD simulation. For the $\alpha_2\beta_2$-heterotetramer, these were supplemented by the 11 structures with the lowest O2–H1 distances (which span the whole 200 ps range and are all at least 5 ps apart), since these shortest distances are statistically too insignificant to be selected by 1 ps sampling. For the purpose of analysing the PESs, the activation energy (E_a) was defined idiosyncratically as the energy difference between the reactant (i.e. the MD snapshot, energy minimized with the value of z restrained) and the top of the barrier; this probably does not correspond to the energy minimum on the reactant side, as illustrated in figure 2*a*. This idiosyncratic E_a can also be thought of as the 'effective barrier height' at 300 K, that is, the potential energy that remains to be overcome subsequent to thermal fluctuations on the PES along the proton-transfer coordinate.

This approach also enables the idiosyncratic E_a to be evaluated as a function of the proton–acceptor distance, d(O2–H1), in both systems (figure 2*b*,*c*). For both systems, E_a for the shortest d(O2–H1) is very similar, suggesting that the difference in rates may not be due to different electrostatic environments of the solvent-exposed active site. In both cases, there is an obvious correlation between E_a and d(O2–H1), although E_a rises much more sharply with d(O2–H1) for the β-monomer. For the $\alpha_2\beta_2$-heterotetramer, E_a follows a concave trend, the dependence of E_a on d(O2–H1) becoming less with increasing d(O2–H1). An explanation for this becomes apparent by analysing individual PESs (figure 3). The reactants with the shortest d(O2–H1) lie part-way up the potential energy barrier (figure 3*a*), with z closer to zero than the minimum on the reactant side, which results in a reduction in the idiosyncratic E_a relative to those structures with a similar minimum z that lie closer to the reactant minimum (figure 3*b*). Conversely, the reactants with the longest d(O2–H1) correspond to reactants that have a more negative z than the reactant minimum (figure 3*c*,*d*). Moving along the PES away from the minimum towards a more negative z does not increase E_a, so these reactants have a similar idiosyncratic E_a to those with a lower d(O2–H1) that lie closer to the energy minimum. That the $\alpha_2\beta_2$-heterotetramer reactant moves along the potential energy profile, both towards and away from the transition state, is further illustrated by comparing the difference in z-value between the reactant and energy minimum on the reactant side with d(O2–H1) (electronic supplementary material, figure S5).

For the β-monomer, on the other hand, the correlation between the idiosyncratic E_a and d(O2–H1) is linear rather than concave. This is suggestive of less motion along the potential energy profile, further supported by comparing the difference in z-value between the reactant and energy minimum on the reactant side for both systems (electronic supplementary material, figure S5). E_a is more heavily dependent on d(O2–H1) than for the $\alpha_2\beta_2$-heterotetramer apparently because the system cannot as easily offset an increase in d(O2–H1) by moving along the barrier at a relatively low energetic cost.

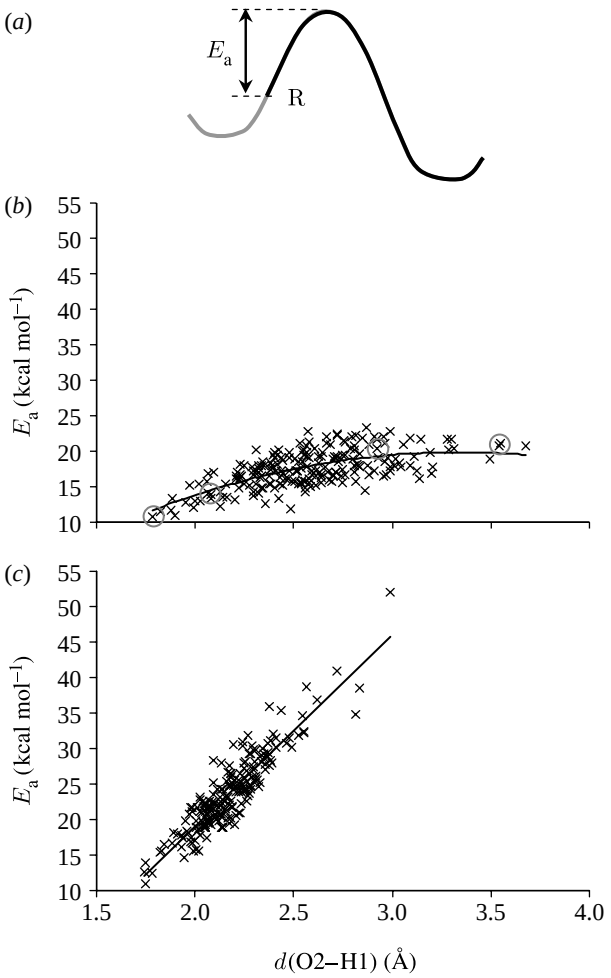

Figure 2. (*a*) Illustration of idiosyncratic activation energy (E_a) used in the analysis, defined as the height from the reactant (R), i.e. the MD snapshot, to the top of the PES; (*b*,*c*) activation energy for proton transfer versus d(O2–H1) for the $\alpha_2\beta_2$-heterotetramer and the β-monomer, respectively. The grey circles indicate the potential energy profiles shown in figure 3.

3.3. The importance of the C1–H1 rotation for proton transfer

The structural changes that occur as the $\alpha_2\beta_2$-heterotetramer system moves along the potential energy profile, rotation of C1–H1 accompanied by a repositioning of O2 (figure 4*a*), corresponds to the approximately 165 cm^{-1} promoting vibration identified previously (Johannissen *et al.* 2007). This is perhaps not surprising, as a promoting vibration is defined as a motion along the reaction coordinate. That the C1–H1 rotation occurs with a 10 kcal mol^{-1} Å^{-2} force constant restraining the MM region, that is, the snapshot from the MD simulation can deviate significantly from the conformation at the energy minimum, supports the previously published conclusion that the approximately 165 cm^{-1} promoting vibration is not part of any large-scale vibrations within the enzyme (Johannissen *et al.* 2007). If this C1–H1 rotation was the result of a 'push' by surrounding residues, then energy minimization of the system at more negative z-values would not be expected to result in a lower energy conformation. Instead, this motion probably arises from an inherent flexibility around the C1 methylene (Johannissen *et al.* 2007).

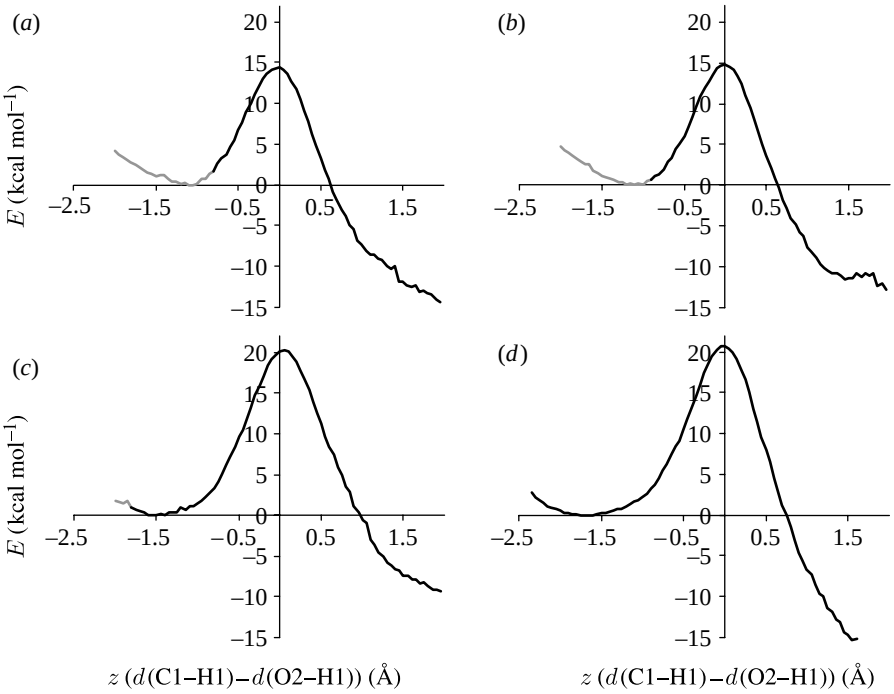

Figure 3. Example potential energy profiles for proton transfer in the $\alpha_2\beta_2$-heterotetramer with the z-value of the MD snapshot (*a*) more positive, (*b*) similar and (*c*,*d*) more negative than the minimum on the reactant side. The black and grey lines represent the potential energy as z increases and z decreases, respectively, from the MD snapshot. The d(O2–H1) distances in the reactant structures are (*a*) 1.78 Å, (*b*) 2.07 Å, (*c*) 2.92 Å and (*d*) 3.54 Å.

The importance of this rotation becomes apparent when comparing the $\alpha_2\beta_2$- and β-reactant structures during typical proton-transfer PES calculations (figure 4). The tunnelling-ready configuration in the $\alpha_2\beta_2$-heterotetramer, with d(O2–H1) approximately 1.6 Å, is achieved by the rotation of C1–H1 towards O2, with a concomitant repositioning of O2 (Masgrau *et al.* 2006). It is probable that a C1–H1 rotation also occurs in the β-monomer (e.g. the DFT frequency calculation for the relaxed iminoquinone analogue shows a 174 cm^{-1} vibration; electronic supplementary material, figure S3), but the C1–H1 orientation corresponding to the minimum energy is similar to that in the tunnelling-ready configuration of the $\alpha_2\beta_2$-heterotetramer, suggesting that this rotation would not bring H1 nearer O2. Instead, decreasing d(O2–H1), and thereby potentially achieving a tunnelling-ready configuration, would require stretching the C1–H1 bond. In other words, while the $\alpha_2\beta_2$-heterotetramer uses the softer bending mode corresponding to the C1–H1 rotation to decrease the O2–H1 distance and achieve a tunnelling-ready configuration, the β-monomer probably employs the stiffer C1–H1 stretching mode.

3.4. Product stabilization in the $\alpha_2\beta_2$-heterotetramer

The $\alpha_2\beta_2$-heterotetramer PESs are all exothermic, while the β-monomer PESs are endothermic or nearly isoenergetic (figure 5). The reason for this difference becomes apparent when comparing structural changes occurring as H1 is transferred from C1 to O2 along typical PESs (figure 6); note that, for the $\alpha_2\beta_2$-heterotetramer, these structural changes are also observed in 50 reactive MD trajectories (Methods in the electronic supplementary material), initiated at z approximately 0 and propagated forwards and backwards in time to the reactant and product (electronic supplementary material, figure S5). The Thr172β Hγ1–Asp128β O2 hydrogen bond is significantly shorter in the β-monomer reactant, which is consistent with the change in conformation of Phe169β which pushes against O2 in the $\alpha_2\beta_2$-heterotetramer; in fact, the Phe169β–O2 distance becomes lower than the sum of carbon and oxygen van der Waals radii during the proton transfer in the $\alpha_2\beta_2$-heterotetramer. The increased C1–O2 distance on the product side of the heterotetramer is accompanied by a breaking of the Thr172β Hγ1–Asp128β O2 hydrogen bond, while in the β-monomer the increased C1–O2 distance on the product side is accompanied by a significant deviation from planarity of the linker region connecting the indole to the quinone (figure 6). This is consistent with previous studies on the analogous enzyme methylamine dehydrogenase, which revealed that proximity of the Asp128β carboxyl to C1–H1 destabilizes the product (Nunez *et al.* 2006) and that the tunnelling reaction is facilitated by increased exothermicity (Nunez *et al.* 2006; Masgrau *et al.* 2007). Thus, Phe169β in the $\alpha_2\beta_2$-heterotetramer facilitates the breakage of the Thr172β–Asp128β hydrogen bond, allowing Asp128β to move further away from C1 and therefore stabilize the product.

3.5. Limitations of this study

Since there is no crystal or NMR structure available for the isolated β-monomer, any differences in this study between the $\alpha_2\beta_2$- and β-forms of AADH are based

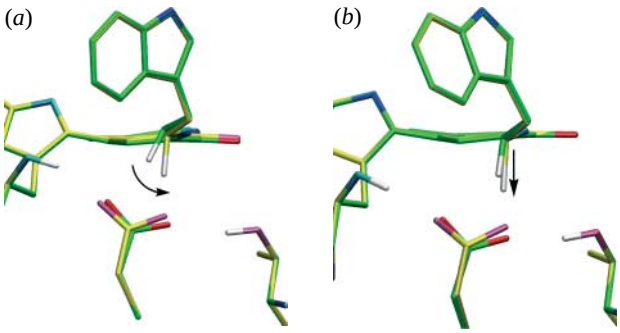

Figure 4. Structural changes occurring during proton transfer in (*a*) the $\alpha_2\beta_2$-heterotetramer and (*b*) the β-monomer. In both panels, the minimum energy reactant structure is shown with green carbon atoms; the $\alpha_2\beta_2$-heterotetramer structure after the maximum degree of C1–H1 rotation is shown with yellow carbon atoms in (*a*), and the β-monomer structure with the corresponding decrease in O2–H1 distance (1.1 Å) is shown with yellow carbon atoms in (*b*) (see also figure 6).

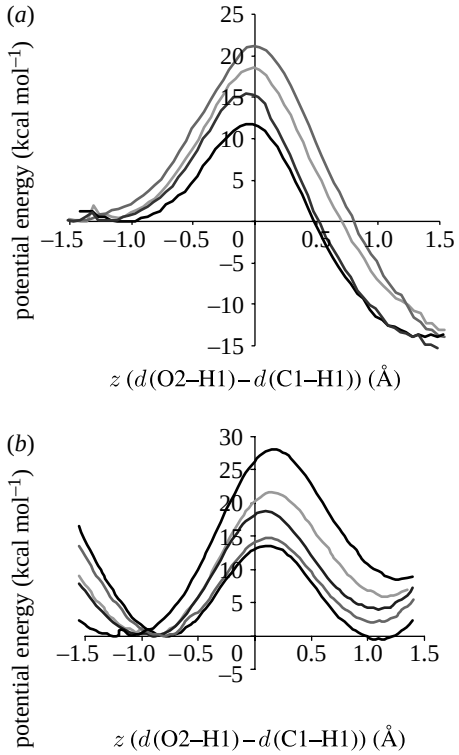

Figure 5. PESs for proton transfer in (*a*) the $\alpha_2\beta_2$-heterotetramer and (*b*) the β-monomer of AADH: tryptamine. Each panel shows the lowest/narrowest to the tallest/widest PESs for the respective structure.

purely on the structural changes that have occurred in the β-monomer during the initial 5 ns of MM MD simulation (which employs the same starting structure as the $\alpha_2\beta_2$-heterotetramer). Thus, we cannot confirm that these are identical to the structural differences between the two forms of AADH in solution, and therefore whether the results of this study unequivocally explain the experimental data. Nevertheless, important insight has been gained from the probable effect of these structural changes on proton transfer, and by implication the important role of the native structure of AADH.

The QM/MM potential energy calculations are carried out using AM1. It is well known that this semi-empirical method overestimates the barrier height relative to *ab initio* and density functional calculations (Nunez *et al.* 2006). However, the purpose of this study is not to produce a quantitative description of the barrier or to reproduce experimental data, but rather to analyse trends in the barriers based on the configuration of the reactant (i.e. the MD snapshot).

A more complete study would require potential of mean force calculations incorporating zero-point energy, excited state and tunnelling contributions using, for example, EA-VTST/MT calculations (Truhlar *et al.* 1985, 2004; Alhambra *et al.* 2001; Gao & Truhlar 2002), an empirical valence bond-based approach (Agarwal *et al.* 2002*a*,*b*; Wong *et al.* 2004) and emerging methods (Jezierska *et al.* 2007).

4. CONCLUSIONS

Key active site features for efficient proton transfer in the rate-limiting step of the oxidative deamination of tryptamine catalysed by AADH have been identified through a QM/MM study. Potential energy barriers for a large sample of reactant structures revealed that a previously identified vibration of the donor methylene group pushes the system along the potential energy profile, thus reducing the effective barrier height and acting as a promoting vibration. This vibration drastically reduces the rate of increase in barrier height with transfer distance in the $\alpha_2\beta_2$-heterotetramer relative to the β-monomer. A specific residue, Phe169β, was found to be essential for product stabilization—a conformational change in this residue in the β-monomer causes the potential energy barriers to go from exothermic to endothermic. Both of these results are qualitatively consistent with the experimentally observed decrease in rate in the β-monomer. This study treats the proton transfer classically, so no direct conclusions can be drawn on the effect of the promoting vibration on the proportion of proton transfers that occur via quantum tunnelling—this vibration lowers the activation energy and will therefore enhance the rate of both over the barrier and tunnelling transfers. Nevertheless, since it has previously been determined that more than 99% of proton transfers in $\alpha_2\beta_2$-heterotetrameric AADH: tryptamine occur by tunnelling, this vibration will increase the *rate* at which tunnelling occurs. In $\alpha_2\beta_2$-heterotetrameric AADH: tryptamine, the iminoquinone is held in a conformation which aligns the main vibration of the donor methylene group with the H-transfer coordinate, allowing thermal fluctuations to bring the system part-way up the potential energy barrier separating the reactant from the product and thus facilitating the reaction.

This work was funded by the UK Biotechnology and Biological Sciences Research Council (BBSRC) and the University of Leicester. N.S.S. is a BBSRC Professorial Research Fellow.

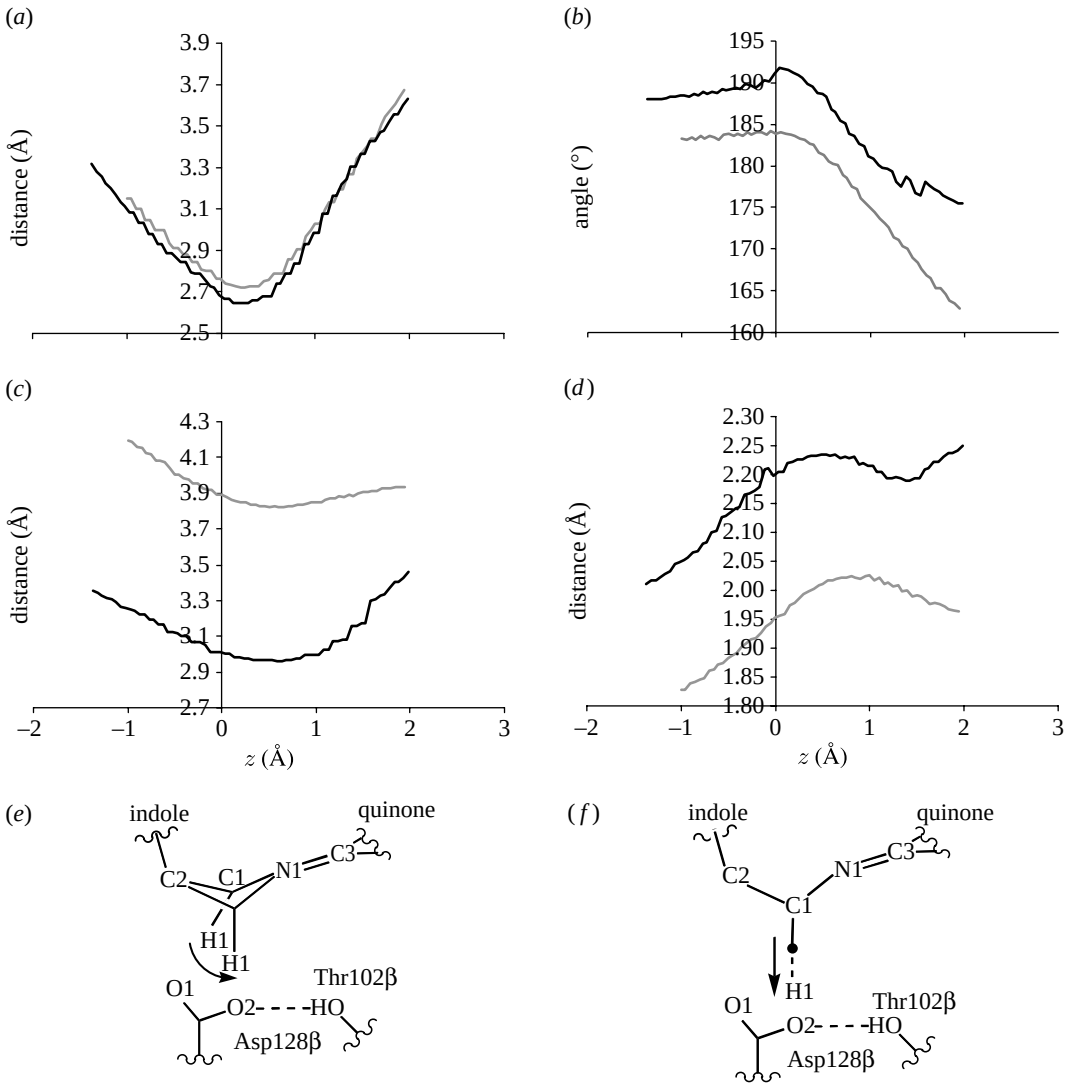

Figure 6. Structural changes occurring during proton transfer in the $\alpha_2\beta_2$-heterotetramer (black lines) and the β-monomer (grey lines) as a function of z, the reaction coordinate: (*a*) C1–O2 distance, (*b*) linker dihedral defined by the C2–C1–N1–C3 angle, (*c*) distance between O2 and nearest carbon on Phe169β, (*d*) O2–Thr102β Hγ1 distance, (*e*) schematic of structural changes in the $\alpha_2\beta_2$-heterotetramer and (*f*) schematic of structural changes in the β-monomer. The arrows in (*e*, *f*) illustrate the proton-transfer coordinate (prior to tunnelling).

REFERENCES

Agarwal, P. K., Billeter, S. R. & Hammes-Schiffer, S. 2002*a* Nuclear quantum effects and enzyme dynamics in dihydrofolate reductase catalysis. *J. Phys. Chem. B* **106**, 3283–3293. (doi:10.1021/jp020190v)

Agarwal, P. K., Billeter, S. R., Rajagopalan, P. T., Benkovic, S. J. & Hammes-Schiffer, S. 2002*b* Network of coupled promoting motions in enzyme catalysis. *Proc. Natl Acad. Sci. USA* **99**, 2794–2799. (doi:10.1073/pnas.052005999)

Alhambra, C., Corchado, J., Sanchez, M. L., Garcia-Viloca, M., Gao, J. & Truhlar, D. G. 2001 Canonical variational theory for enzyme kinetics with the protein mean force and multidimensional quantum mechanical tunneling dynamics. Theory and application to liver alcohol dehydrogenase. *J. Phys. Chem. B* **105**, 11 326–11 340. (doi:10.1021/jp0120312)

Ball, P. 2004 Enzymes: by chance, or by design? *Nature* **431**, 396–397. (doi:10.1038/431396a)

Benkovic, S. J. & Hammes-Schiffer, S. 2003 A perspective on enzyme catalysis. *Science* **301**, 1196–1202. (doi:10.1126/science.1085515)

Billeter, S. R., Webb, S. P., Agarwal, P. K., Iordanov, T. & Hammes-Schiffer, S. 2001 Hydride transfer in liver alcohol dehydrogenase: quantum dynamics, kinetic isotope effects, and role of enzyme motion. *J. Am. Chem. Soc.* **123**, 11 262–11 272. (doi:10.1021/ja011384b)

Brooks, B. R., Bruccoleri, R. E., Olafson, B. D., States, D. J., Swaminathan, S. & Karplus, M. 1983 CHARMM—a program for macromolecular energy, minimization, and dynamics calculations. *J. Comput. Chem.* **4**, 187–217. (doi:10.1002/jcc.540040211)

Caratzoulas, S., Mincer, J. S. & Schwartz, S. D. 2002 Identification of a protein-promoting vibration in the reaction catalyzed by horse liver alcohol dehydrogenase. *J. Am. Chem. Soc.* **124**, 3270–3276. (doi:10.1021/ja017146y)

Cui, Q. & Karplus, M. 2002 Quantum mechanics/molecular mechanics studies of triosephosphate isomerase-catalyzed reactions: effect of geometry and tunneling on proton-transfer rate constants. *J. Am. Chem. Soc.* **124**, 3093–3124. (doi:10.1021/ja0118439)

Dybala-Defratyka, A., Paneth, P., Banerjee, R. & Truhlar, D. G. 2007 Coupling of hydrogenic tunneling to active-site

motion in the hydrogen radical transfer catalyzed by a coenzyme B12-dependent mutase. *Proc. Natl Acad. Sci. USA* **104**, 10 774–10 779. (doi:10.1073/pnas.0702188104)

Field, M. J., Bash, P. A. & Karplus, M. 1990 A combined quantum-mechanical and molecular mechanical potential for molecular-dynamics simulations. *J. Comput. Chem.* **11**, 700–733. (doi:10.1002/jcc.540110605)

Gao, J. & Truhlar, D. G. 2002 Quantum mechanical methods for enzyme kinetics. *Annu. Rev. Phys. Chem.* **53**, 467–505. (doi:10.1146/annurev.physchem.53.091301.150114)

Garcia-Viloca, M., Alhambra, C., Truhlar, D. G. & Gao, J. 2001 Inclusion of quantum-mechanical vibrational energy in reactive potentials of mean force. *J. Chem. Phys.* **114**, 9953–9958. (doi:10.1063/1.1371497)

Garcia-Viloca, M., Truhlar, D. G. & Gao, J. 2003 Reaction-path energetics and kinetics of the hydride transfer reaction catalyzed by dihydrofolate reductase. *Biochemistry* **42**, 13 558–13 575. (doi:10.1021/bi034824f)

Hammes-Schiffer, S. 2006 Hydrogen tunneling and protein motion in enzyme reactions. *Acc. Chem. Res.* **39**, 93–100. (doi:10.1021/ar040199a)

Hay, S., Sutcliffe, M. J. & Scrutton, N. S. 2007 Promoting motions in enzyme catalysis probed by pressure studies of kinetic isotope effects. *Proc. Natl Acad. Sci. USA* **104**, 507–512. (doi:10.1073/pnas.0608408104)

Henzler-Wildman, K. & Kern, D. 2007 Dynamic personalities of proteins. *Nature* **450**, 964–972. (doi:10.1038/nature06522)

Hothi, P., Lee, M., Cullis, P. M., Leys, D. & Scrutton, N. S. 2008 Catalysis by the isolated tryptophan tryptophylquinone-containing subunit of aromatic amine dehydrogenase is distinct from native enzyme and synthetic model compounds and allows further probing of TTQ mechanism. *Biochemistry* **47**, 183–194. (doi:10.1021/bi701690u)

Jezierska, A., Panek, J. J., Koll, A. & Mavri, J. 2007 Car–Parrinello simulation of an O–H stretching envelope and potential of mean force of an intramolecular hydrogen bonded system: application to a Mannich base in solid state and in vacuum. *J. Chem. Phys.* **126**, 205 101–205 109. (doi:10.1063/1.2736692)

Johannissen, L. O., Hay, S., Scrutton, N. S. & Sutcliffe, M. J. 2007 Proton tunneling in aromatic amine dehydrogenase is driven by a short-range sub-picosecond promoting vibration: consistency of simulation and theory with experiment. *J. Phys. Chem. B* **111**, 2631–2638. (doi:10.1021/jp066276w)

Knapp, M. J., Rickert, K. & Klinman, J. P. 2002 Temperature-dependent isotope effects in soybean lipoxygenase-1: correlating hydrogen tunneling with protein dynamics. *J. Am. Chem. Soc.* **124**, 3865–3874. (doi:10.1021/ja012205t)

Kohen, A. 2006 Current issues in enzymatic hydrogen transfer from carbon: tunneling and coupled motion from kinetic isotope effect studies. In *Hydrogen transfer reactions*, vol. 4 (eds J. T. Hynes, J. P. Klinman, H. H. Limbach & R. L. Schowen), pp. 1311–1340. Weinheim, Germany: Wiley.

Liu, H. & Warshel, A. 2007*a* The catalytic effect of dihydrofolate reductase and its mutants is determined by reorganization energies. *Biochemistry* **46**, 6011–6025. (doi:10.1021/bi700201w)

Liu, H. & Warshel, A. 2007*b* Origin of the temperature dependence of isotope effects in enzymatic reactions: the case of dihydrofolate reductase. *J. Phys. Chem. B* **111**, 7852–7861. (doi:10.1021/jp070938f)

Masgrau, L. *et al.* 2006 Atomic description of an enzyme reaction dominated by proton tunneling. *Science* **312**, 237–241. (doi:10.1126/science.1126002)

Masgrau, L., Ranaghan, K. E., Scrutton, N. S., Mulholland, A. J. & Sutcliffe, M. J. 2007 Tunneling and classical paths for proton transfer in an enzyme reaction dominated by tunneling: oxidation of tryptamine by aromatic amine dehydrogenase. *J. Phys. Chem. B* **111**, 3032–3047. (doi:10.1021/jp067898k)

Nunez, S., Tresadern, G., Hillier, I. H. & Burton, N. A. 2006 An analysis of reaction pathways for proton tunnelling in methylamine dehydrogenase. *Phil. Trans. R. Soc. B* **361**, 1387. (doi:10.1098/rstb.2006.1867)

Olsson, M. H., Mavri, J. & Warshel, A. 2006*a* Transition state theory can be used in studies of enzyme catalysis: lessons from simulations of tunnelling and dynamical effects in lipoxygenase and other systems. *Phil. Trans. R. Soc. B* **361**, 1417–1432. (doi:10.1098/rstb.2006.1880)

Olsson, M. H., Parson, W. W. & Warshel, A. 2006*b* Dynamical contributions to enzyme catalysis: critical tests of a popular hypothesis. *Chem. Rev.* **106**, 1737–1756. (doi:10.1021/cr040427e)

Pang, J., Pu, J., Gao, J., Truhlar, D. G. & Allemann, R. K. 2006 Hydride transfer reaction catalyzed by hyperthermophilic dihydrofolate reductase is dominated by quantum mechanical tunneling and is promoted by both inter- and intramonomeric correlated motions. *J. Am. Chem. Soc.* **128**, 8015–8023. (doi:10.1021/ja061585l)

Pang, J., Hay, S., Scrutton, N. S. & Sutcliffe, M. J. 2008 Deep tunneling dominates the biologically important hydride transfer reaction from NADH to FMN in morphinone reductase. *J. Am. Chem. Soc.* **130**, 7092–7097. (doi:10.1021/ja800471f)

Pu, J., Gao, J. & Truhlar, D. G. 2006 Multidimensional tunneling, recrossing, and the transmission coefficient for enzymatic reactions. *Chem. Rev.* **106**, 3140–3169. (doi:10.1021/cr050308e)

Sutcliffe, M. J. & Scrutton, N. S. 2006 Computational studies of enzyme mechanism: linking theory with experiment in the analysis of enzymic H-tunnelling. *Phys. Chem. Chem. Phys.* **8**, 4510–4516. (doi:10.1039/b609622k)

Tejero, I., Garcia-Viloca, M., Gonzalez-Lafont, A., Lluch, J. M. & York, D. M. 2006 Enzyme dynamics and tunneling enhanced by compression in the hydrogen abstraction catalyzed by soybean lipoxygenase-1. *J. Phys. Chem. B* **110**, 24 708–24 719. (doi:10.1021/jp066263i)

Truhlar, D. G., Isaacson, A. D. & Garret, B. C. 1985 Generalized transition state theory. In *Theory of chemical reaction dynamics*, vol. IV (ed. M. Baer), pp. 65–136. Boca Raton, FL: CRC Press.

Truhlar, D. G., Gao, J. L., Garcia-Viloca, M., Alhambra, C., Corchado, J., Sanchez, M. L. & Poulsen, T. D. 2004 Ensemble-averaged variational transition state theory with optimized multidimensional tunneling for enzyme kinetics and other condensed-phase reactions. *Int. J. Quant. Chem.* **100**, 1136–1152. (doi:10.1002/qua.20205)

Wand, A. J. 2001 Dynamic activation of protein function: a view emerging from NMR spectroscopy. *Nat. Struct. Biol.* **8**, 926–931. (doi:10.1038/nsb1101-926)

Warshel, A. 1998 Electrostatic origin of the catalytic power of enzymes and the role of preorganized active sites. *J. Biol. Chem.* **273**, 27 035–27 038. (doi:10.1074/jbc.273.42.27035)

Wong, K. F., Watney, J. B. & Hammes-Schiffer, S. 2004 Analysis of electrostatics and correlated motions for hydride transfer in dihydrofolate reductase. *J. Phys. Chem. B* **108**, 12 231–12 241. (doi:10.1021/jp048565v)

Yon, J. M., Perahia, D. & Ghelis, C. 1998 Conformational dynamics and enzyme activity. *Biochimie* **80**, 33–42. (doi:10.1016/S0300-9084(98)80054-0)